

Published in final edited form as:

Sci Signal. ; 4(202): ra84. doi:10.1126/scisignal.2002058.

Protein Kinase C η is Required for T Cell Activation and Homeostatic Proliferation

Guo Fu^{1,*}, Jianfang Hu^{1,†}, Nathalie Niederberger-Magnenat^{1,2,†,‡}, Vasily Rybakin¹, Javier Casas¹, Pia P. Yachi^{1,§}, Stephanie Feldstein^{1,||}, Bo Ma^{3,§}, John A. H. Hoerter¹, Jeanette Ampudia¹, Stephanie Rigaud¹, Florence Lambolez², Amanda L. Gavin^{1,¶}, Karsten Sauer¹, Hilde Cheroutre², and Nicholas R. J. Gascoigne^{1,*}

¹Department of Immunology and Microbial Science, The Scripps Research Institute, 10550 North Torrey Pines Road, La Jolla, CA 92037, USA.

²Department of Developmental Immunology, La Jolla Institute for Allergy and Immunology, 9420 Athena Circle, La Jolla, CA 92037, USA.

³Department of Molecular and Experimental Medicine, The Scripps Research Institute, 10550 North Torrey Pines Road, La Jolla, CA 92037, USA.

Abstract

Protein kinase C η (PKC η) is highly abundant in T cells and is recruited to the immunological synapse that is formed between a T cell and a cognate antigen-presenting cell; however, its function in T cells is unknown. Here, we showed that PKC η was required for the activation of mature CD8⁺ T cells by stimulation through the T cell receptor. PKC η ^{-/-} T cells showed poor proliferation in response to stimulation by antigen as compared to wild-type T cells, a trait shared with T cells deficient in PKC θ , the most abundant PKC isoform in T cells, and the only PKC previously thought to have a specific role in T cell activation. In contrast, defective homeostatic proliferation, a function requiring recognition of self antigens, was only observed in PKC η -deficient T cells. PKC η was dispensable for the development of thymocytes; however, thymocytes from mice doubly deficient in PKC η and PKC θ exhibited poor positive selection, indicating some redundancy between the PKC isoforms. PKC η and PKC θ had opposing effects on relative numbers of CD4⁺ and CD8⁺ T cells, because PKC η ^{-/-} mice had a higher ratio of CD4⁺ to CD8⁺ T cells compared to that of wild-type mice, whereas PKC θ ^{-/-} mice had a lower ratio. In mice deficient in both PKC isoforms, the ratio of CD4⁺ to CD8⁺ T cells returned to normal. Together, these data suggest that whereas PKC η shares redundant roles with PKC θ in T cell biology, it also performs nonredundant functions that are important for homeostasis and activation of T cells.

*To whom correspondence should be addressed. gascoigne@scripps.edu (N.R.J.G.); guofu@scripps.edu (G.F.) .

†These authors contributed equally to this work.

‡Current address: Faculty of Biology and Medicine, University of Lausanne, Switzerland.

§Current address: Applied Molecular Evolution, 3520 Dunhill Street, San Diego, CA 92121, USA.

||Current address: School of Medicine, University of California San Diego, 9500 Gilman Drive, La Jolla, CA 92093, USA.

¶Current address: Burnet Institute, 85 Commercial Rd., Melbourne, Victoria, Australia 3004.

Author contributions: G.F. and N.R.J.G. designed the project; G.F. made the knockout mice with help from B.M.; G.F., J.H., A.L.G., F.L., S.F., H.C., J.A.A.H., and J.A. analyzed the mice; V.R., S.R. and K.S. performed or analyzed biochemical experiments; G.F., J.C., P.P.Y., and N.N.-M. performed imaging; N.N.-M. made the initial finding that PKC η abundance was increased during thymocyte development; and G.F. and N.R.J.G. wrote the manuscript.

Competing interests: The authors declare that they have no competing interests.

INTRODUCTION

The protein kinase C (PKC) family of serine and threonine kinases includes 10 isoforms in human and mouse, which play important roles in signal transduction in different cellular systems, including regulating differentiation, cell motility, secretion, growth and death (1). Of the PKC isoforms found in T cells (α , δ , ϵ , η , and θ), only PKC θ is thought to have an important and specific role in T cell biology, where it is involved in costimulation of signal transduction in response to antigen recognition, leading to activation of transcription factors including NF- κ B and to changes in gene transcription resulting in responses such as increased IL-2 secretion (2-5). However, PKC η gene expression is increased during positive selection (6, 7), and gene expression profiling has shown that PKC η messenger RNA (mRNA) abundance, like that of PKC θ , is higher in T cells than in other mouse or human cell types and organs (<http://biogps.org/#goto=genereport&id=18755;gnf1m00727> and U133A 206099_at) which suggests that PKC η may play a role in T cell biology. Although a PKC η -deficient mouse exists, no immunological studies of these mice have been reported (8).

PKC θ is recruited to the immunological synapse, the area of contact that is formed between mature T cells and antigen-presenting cells (APCs), where it concentrates in the central region (9-11). In addition, PKC θ associates with the coreceptor CD28 in microclusters that contain the T cell antigen receptor (TCR), which move centripetally into the immunological synapse and are thought to be important in the costimulation of T cells (12). A fusion protein of PKC η and green fluorescent protein (GFP) is also recruited to the immunological synapse upon TCR stimulation, where it is localized diffusely over the whole region (13). Studies with PKC $\theta^{-/-}$ mice revealed the involvement of PKC θ in multiple signaling pathways downstream of TCR stimulation (14-20). Given the importance of PKC θ in mature T cells, it was surprising that initial studies showed no defect in T cell development in PKC $\theta^{-/-}$ mice (14, 16); however, another study found that PKC θ is indeed involved in thymocyte development, with PKC $\theta^{-/-}$ mice showing a mild defect in positive selection (21). Redundancy between different PKC isoforms may obscure the importance of any individual PKC in T cell development and function in vivo.

Here, we confirmed that the abundance of PKC η mRNA is increased during the positive selection of thymocytes, and we found that PKC η , similar to PKC θ , was recruited to the immunological synapse. To further investigate the specific role of PKC η and the potential redundancy between PKC η and PKC θ in T cell development and mature T cell function, we generated mice deficient in *Prkch*, the gene encoding PKC η (PKC $\eta^{-/-}$ mice), and mice doubly deficient in *Prkch* and *Prckq*, which encodes PKC θ , to generate PKC $\eta^{-/-}$ PKC $\theta^{-/-}$ double knockout (DKO) mice. We found that although PKC η shared redundant functions with PKC θ during T cell development, PKC η was required for normal functions of mature T cells, because PKC $\eta^{-/-}$ T cells were less well able to proliferate in response to antigen or to undergo homeostatic proliferation than were wild-type mice, which was likely a result of impaired intracellular calcium (Ca²⁺) signaling and nuclear translocation of the transcription factor nuclear factor κ B (NF- κ B), defects similar to those found in PKC $\theta^{-/-}$ mice. In contrast to PKC $\eta^{-/-}$ and PKC $\theta^{-/-}$ mice, DKO mice had a more severe defect in T cell development and more profound functional defects in mature T cells, as was revealed in multiple assays. Together, our data suggest that in addition to sharing redundant roles with PKC θ , PKC η has its own specific functions in T cell biology.

RESULTS

The abundance of PKC η mRNA is increased during positive selection of thymocytes

In a previous study, we showed that the abundance of PKC η mRNA is increased in pre-selection thymocytes when stimulated with an antibody against the V β chain of TCR (7). Independently, Hogquist and colleagues also found that PKC η mRNA abundance is increased during positive selection (6). Given the requirement for PKC θ for antigenic stimulation in mature T cells (9, 10, 14, 16), it was surprising that PKC η rather than PKC θ mRNA abundance was increased during positive selection (7). To investigate whether PKC η was involved in thymocyte positive selection *in vivo*, and to test whether PKC η might compensate for the loss of PKC θ , we measured PKC η mRNA amounts by real-time reverse transcription polymerase chain reaction (RT-PCR) assay. We found that PKC η mRNA was increased in abundance in late-stage CD4⁺ and CD8⁺ double-positive (DP) cells and in CD4⁺ single-positive (SP) and CD8⁺ SP cells, that is, in cells that had undergone positive selection (Fig. 1A, left). DP cells with a high abundance of TCR as assessed by flow cytometry (TCR^{hi} DP cells) showed about a four-fold increase in PKC η mRNA abundance compared to that in TCR^{lo} DPs, and this abundance stayed high in the SP cells. Because PKC θ is found in earlier developmental stages in thymocytes than PKC η , if there was redundancy between the PKC θ and PKC η isoforms, we would expect that PKC η would be produced earlier in cells in the absence of PKC θ . Indeed, we found that expression of the gene encoding PKC η was induced earlier and to a greater extent than normal in cells before positive selection (TCR^{lo} DP cells) (Fig. 1A, right). These results suggested that PKC η might play a role in thymocyte development.

PKC η is recruited to the immunological synapse

Because the gene encoding PKC η was induced during normal positive selection and because it was expressed earlier and to a greater extent in PKC θ ^{-/-} thymocytes than in wild-type thymocytes, we tested whether PKC η , like PKC θ , was recruited to the immunological synapse in thymocytes. The recruitment of PKC θ to the synapse is important in signal transduction and is a hallmark of recognition of antigenic peptide presented by major histocompatibility complex (MHC). To avoid the possibility of cross-reaction between antibodies against PKC η and PKC θ , we first isolated thymocytes and mature T cells from PKC θ ^{-/-} mice and activated them with APCs that presented the superantigens staphylococcal enterotoxin A (SEA) and SEB, which react with more than 40% of the V β repertoire of TCRs in B6 mice (22). Superantigens like SEA and SEB bind to MHC class II molecules and are then able to activate T cells by binding to the TCR through recognition of V β sequences. PKC η was recruited to the immunological synapse in thymocytes and in mature T cells upon stimulation with SEA and SEB (Fig. 1B). In PKC θ -sufficient thymocytes, PKC θ , but not PKC η , was present at the immunological synapse of DP cells before selection (PKC η is not yet present in these cells) (fig. S1). In SP cells, both PKC θ and PKC η were found at the immunological synapse. In PKC θ ^{-/-} thymocytes, PKC η mRNA was detected in less mature DP cells than in wild-type thymus (Fig. 1A), and consequently PKC η was present in the immunological synapses of DP cells (fig. S2).

To visualize the recruitment of PKC η to the immunological synapse in live cells, we transfected OT-I hybridoma cells (23), that have a TCR that recognizes a peptide from ovalbumin (OVA) presented on the MHC class I-molecule H2-K^b, with plasmids encoding mouse PKC η fused to red fluorescent protein (PKC η -RFP) or PKC θ -RFP. We stimulated these cells with EL4 cells that had been incubated ("pulsed") with different peptides. When the stimulatory OVA peptide was presented to the OT-I cells, both PKC η and PKC θ were recruited to the immunological synapse; however, when the nonstimulatory vesicular stomatitis virus (VSV) peptide was presented, no such recruitment took place, which

demonstrated that the recruitment of PKC η to the immunological synapse was antigen-specific (Fig. 1C). Genes for GFP tagged human PKC η , θ and α proteins were transfected into human Jurkat T cells (fig. S3A). PKC η and θ , but not PKC α , were recruited to the immunological synapse during recognition of a superantigen ligand. Similarly, stimulation of an MHC class II-restricted T cell hybridoma with antigenic peptide-pulsed APC, resulted in concentration of transgenic fluorescent-tagged PKC η and θ , but not PKC δ at the synapse (fig. S3B). To compare the recruitment of PKC η and PKC θ directly, we cotransfected OT-I cells with plasmids encoding PKC η -RFP and PKC θ -GFP and imaged the fluorescent proteins during antigen recognition (fig. S4). Both PKC η and PKC θ were recruited to the immunological synapse; however, whereas PKC η remained in a diffuse pattern over the whole area of the synapse (Fig. 1, B and C), which was consistent with an earlier study (13), PKC θ was more centrally concentrated at the immunological synapse (Fig. 1, B and C), as was expected from previous work (9, 10).

PKC η is not required for positive or negative selection of thymocytes

To investigate the role of PKC η in a broader manner, we generated *Prkch*-deficient (PKC $\eta^{-/-}$) mice (fig. S5). The thymi of PKC $\eta^{-/-}$ mice contained ~20% fewer cells than did the thymi of wild-type mice. When we analyzed thymocyte subsets in the thymi of PKC $\eta^{-/-}$ mice, we found that the numbers of double-negative (DN1) and DN4 cells were reduced compared to those in thymi from wild-type mice; however, the numbers of DN2 and DN3 cells were not altered (Fig. 2A). DN4 cells develop into CD4⁺CD8⁺ DP cells, after which they are subjected to positive and negative selection to generate self-MHC-restricted, self-antigen-tolerant mature T cells (24). The proportions of DP, CD4⁺ SP, and CD8⁺ SP subsets were similar in the thymi of PKC $\eta^{-/-}$ and wild-type mice, with slightly reduced cell numbers of DP subsets in the PKC $\eta^{-/-}$ mice (Fig. 2B). These results suggested that PKC η was not required for the positive selection of thymocytes.

To investigate the role of PKC η in negative selection, we used a superantigen-mediated deletion model. Mouse mammary tumor proviruses encode superantigens (Mtv) that are presented by the MHC class II molecule I-E to T cells, resulting in the intrathymic deletion of cells bearing V β elements recognized by particular Mtv superantigens (22, 25). Because B6 (MHC haplotype H-2^b) mice do not express I-E, we crossed the B6 PKC $\eta^{-/-}$ mice to B10.D2 (H-2^d) mice, producing F1 H-2^{b/d} mice that express I-E^d. In combination with the endogenous superantigens Mtv-8 and Mtv-9, which are carried by both B6 and B10.D2 cells, I-E causes the deletion of thymocytes that express the V β 5, V β 11, and V β 12 chains of the TCR on their surface (22, 25). When we compared H-2^{b/b} mice with H-2^{b/d} PKC $\eta^{+/+}$ mice, we found that a substantial number of T cells expressing V β 5, V β 11, and V β 12 TCRs were deleted in the H-2^{b/d}, I-E expressing F1 mice (Fig. 2C). V β 7⁺ T cells do not recognize Mtv-8 and Mtv-9 superantigens and thus were not deleted in either mouse. Superantigen-mediated negative selection was as efficient in the H-2^{b/d} PKC $\eta^{-/-}$ as PKC $\eta^{+/+}$ mice, indicating that PKC η was dispensable for superantigen-mediated negative selection.

Increased number of memory phenotype T cells in PKC η -deficient mice

We observed that the lymph nodes of PKC $\eta^{-/-}$ mice were larger than those of wild-type mice (Fig. 3A). In the cervical area there were more and larger readily identifiable lymph nodes in PKC $\eta^{-/-}$ mice than in wild-type mice (Fig. 3A, left). When we isolated the axillar, brachial, and inguinal lymph nodes, we found that they were larger in PKC $\eta^{-/-}$ mice than in wild-type mice (Fig. 3A, right). Consistent with this finding, the number of lymph node cells was increased in the PKC $\eta^{-/-}$ mice compared to that in the wild-type mice (Fig. 3B). These data suggested that PKC $\eta^{-/-}$ mice may have a general over-production of lymphocytes rather than swollen lymph nodes (lymphadenopathy); however, the number of lymphocytes in the spleens of PKC $\eta^{-/-}$ mice was less than that of wild-type mice (Fig. 3B). In the lymph

nodes, although there were only minor changes in the proportions of T cells or B cells or in the T cell subpopulations [CD8⁺, CD4⁺CD25⁻ conventional CD4⁺ cells, or CD4⁺CD25⁺ regulatory T cells (T_{regs})] (Fig. 3C), the absolute number of each cell type was substantially increased in the PKC η ^{-/-} mice compared to those in wild-type mice (Fig. 3D), whereas the numbers of each cell type were lower in the spleens of PKC η ^{-/-} mice than in those of wild-type mice. The proportion of cells with a memory or activated phenotype within the conventional CD4⁺CD25⁻ population (CD44⁺) of cells was increased in the lymph nodes and the spleens of PKC η ^{-/-} mice compared to those in wild-type mice (Fig. 3, C and D). We obtained similar results when we used the transcription factor Foxp3, rather than the surface marker CD25, to define T_{regs} (fig. S6, A and B). The total numbers of lymph node and splenic lymphocyte subsets were very similar in wild type and PKC η ^{-/-} mice, which suggested that the lymphocytes of PKC η -deficient mice might preferentially home to the lymph nodes rather than to the spleen. The exception to this conservation in total lymphocyte number in the secondary lymphoid tissues was the decrease in the total number of naïve CD4⁺CD25⁻ and the increase in the number of CD4⁺CD25⁻ memory phenotype T cells in the PKC η ^{-/-} mice compared to those of wild-type mice, suggesting that the knockout cells may have responded to more self-stimulation in the periphery than the wild-type cells (26).

PKC η -deficient T cells show impaired proliferation

To test the proliferative response of PKC η ^{-/-} T cells, we purified naïve CD4⁺ or CD8⁺ T cells from lymph nodes, stimulated them through the TCR with various concentrations of antibody against CD3, and measured their proliferative responses. Naïve CD4⁺ and CD8⁺ T cells from PKC η ^{-/-} mice proliferated less well than did naïve CD4⁺ and CD8⁺ T cells from wild-type mice (Fig. 4A). Unlike PKC θ ^{-/-} CD8⁺ T cells whose proliferation was completely abrogated by loss of PKC θ , the proliferation of PKC η ^{-/-} CD8⁺ T cells was only moderately reduced by 30 to 50% (Fig. 4A). So that both cell types could experience an identical cytokine environment, we determined cell division by measuring the dilution of the cytoplasmic dye carboxyfluorescein succinimidyl ester (CFSE) with a mixture of PKC η ^{-/-} T cells (which had the surface marker CD45.2) and PKC η ^{+/+} T cells (which had the surface marker CD45.1). CD8⁺ T cells from PKC η ^{-/-} mice proliferated less well than did PKC η ^{+/+} cells in response to stimulation by antibody against CD3 or by crosslinking of T cell surface glycoproteins with the lectin concanavalin A (ConA) (Fig. 4B). We then performed a similar experiment with MHC class I-restricted OT-I TCR transgenic T cells that responded to different concentrations of OVA peptide presented by splenic APCs. In these experiments, PKC η ^{-/-} or PKC θ ^{-/-} T cells (which had the surface marker Thy1.2) were mixed with PKC η ^{+/+} T cells (which had the surface marker Thy1.1). The PKC η ^{-/-} T cells proliferated more weakly than did the PKC η ^{+/+} cells, but more strongly than did the PKC θ ^{-/-} cells (Fig. 4C).

To investigate the proliferation of PKC η ^{-/-} T cells under more physiological conditions, we stimulated OT-I TCR transgenic PKC η ^{-/-} T cells *in vivo* with bone marrow-derived dendritic cells (BMDCs) that were loaded with OVA peptide. We purified wild-type (Thy1.1⁺CD45.2⁺) and PKC η ^{-/-} (Thy1.2⁺CD45.2⁺) OT-I T cells from lymph nodes, mixed the cells at a 1:1 ratio, and injected them into recipient mice that had been immunized with OVA-loaded BMDCs one day before the experiment (Fig. 4D). The proportional contribution of each donor cell type to the total population of cells was determined at various time points by flow cytometric analysis (Fig. 4D). Both types of donor cell proliferated in the recipient mice, reaching their peak numbers on day 4, after which they declined (Fig. 4E). However, although both types of donor cells proliferated with similar kinetics, their respective proliferative capacities were quite different. The proportions of PKC η ^{+/+} and PKC η ^{-/-} T cells within the donor population started to diverge on day 1 (Fig.

4F). This difference in proportions increased over time, peaking at day 3, at which point the percentages of wild-type and PKC $\eta^{-/-}$ T cells were 69 versus 30%. This difference in cellular proportions was maintained until the end of the experiment. The differences in the proportion of PKC $\eta^{+/+}$ T cells to PKC $\eta^{-/-}$ T cells could have occurred because of differential cell death between the populations. To test this possibility, we incubated donor cells with labeled Annexin V to detect cell surface phosphatidylserine (present on early apoptotic cells) and the DNA-intercalating dye 7-AAD to distinguish viable from dying cells. Both PKC $\eta^{+/+}$ and PKC $\eta^{-/-}$ T cells had a small and roughly equal subset of dying cells (fig. S7), which suggested that differential cell death was unlikely to contribute to the difference in cellular proportions observed earlier (Fig. 4F). Collectively, these data indicate that the PKC $\eta^{-/-}$ CD8 $^{+}$ T cells had a defect in the proliferative response to TCR stimulation, although the defect that was observed in assays in vitro was milder than that seen in PKC $\theta^{-/-}$ T cells.

Ca $^{2+}$ and NF- κ B signaling in PKC η -deficient T cells are defective

The proliferative defect in PKC $\eta^{-/-}$ T cells could be a result of insufficient production of the cytokine interleukin-2 (IL-2), a prosurvival factor for T cells, deficient synthesis of the α chain of the IL-2 receptor (IL-2R α , also known as CD25), or both, as occurs in PKC $\theta^{-/-}$ T cells (14, 16). In PKC $\eta^{-/-}$ CD8 $^{+}$ cells, the increase in the cell-surface abundance of CD25 was substantially reduced compared to that in wild-type CD8 $^{+}$ cells, similar to the reduction in PKC $\theta^{-/-}$ T cells (16) (Fig. 5A), as was the increase in abundance of the early activation marker CD69 (Fig. 5B). Because CD4 $^{+}$ T cells are the main source of IL-2, we measured the amount of IL-2 secreted by PKC $\eta^{-/-}$ CD4 $^{+}$ T cells and found that it was slightly (but significantly) reduced compared to that of wild-type CD4 $^{+}$ T cells (fig. S8A).

NF- κ B and Ca $^{2+}$ signaling pathways are defective in PKC $\theta^{-/-}$ mice, whereas TCR-proximal and mitogen-activated protein kinase (MAPK) signaling pathways are intact (14, 16, 20). We therefore investigated these pathways to try to determine the potential mechanisms responsible for the defects that we observed in PKC $\eta^{-/-}$ T cells. To measure changes in Ca $^{2+}$ flux, we mixed wild-type (Thy1.1 $^{+}$) and PKC $\eta^{-/-}$ (Thy1.2 $^{+}$) T cells, loaded them with the Ca $^{2+}$ -indicator dye Indo-1, and stimulated their TCRs by crosslinking prebound antibodies against CD3. In the PKC η -sufficient CD8 $^{+}$ T cells, we observed a transient peak of elevated Ca $^{2+}$ followed by a sustained, gradually declining, Ca $^{2+}$ signal. In PKC $\eta^{-/-}$ CD8 $^{+}$ T cells, the magnitude of the Ca $^{2+}$ signal was reduced. This difference in Ca $^{2+}$ signaling was not because of differential Indo-1 loading, because both cell types exhibited equivalent signals when stimulated with the Ca $^{2+}$ ionophore ionomycin (Fig. 5C). Ca $^{2+}$ signaling includes both the release of Ca $^{2+}$ from endoplasmic reticulum (ER) stores and the subsequent induction of store-operated Ca $^{2+}$ entry (SOCE) through channels in the plasma membrane (27). To identify at which stage Ca $^{2+}$ signals were affected in PKC $\eta^{-/-}$ T cells, we measured Ca $^{2+}$ flux in cells incubated with EGTA, which chelates extracellular Ca $^{2+}$, thus enabling us to measure only ER-dependent Ca $^{2+}$ release, and in cells that were subsequently replenished with extracellular Ca $^{2+}$, thus enabling us to measure SOCE. These experiments showed no defect in ER-dependent Ca $^{2+}$ release but did reveal a defect in SOCE in PKC $\eta^{-/-}$ T cells (Fig. 5D). We then directly compared Ca $^{2+}$ signaling in PKC $\eta^{-/-}$ CD8 $^{+}$ T cells and PKC $\theta^{-/-}$ CD8 $^{+}$ T cells and found a similar defect (fig. S8B).

The translocation of the NF- κ B p65 subunit from the cytosol to the nucleus is a hallmark event in the NF- κ B signaling cascade. We stimulated purified CD8 $^{+}$ T cells with crosslinked antibodies against CD3 and CD8 and imaged the nuclear and cytoplasmic localization of p65. We observed translocation of p65 to the nucleus of 40% of wild-type cells, but only in 22% of PKC $\theta^{-/-}$ T cells, whereas only 15% of PKC $\eta^{-/-}$ T cells showed nuclear translocation of p65 (Fig. 5, E and F). This result was further confirmed by Western blotting analysis of cytosolic and nuclear extracts. In wild-type CD8 $^{+}$ T cells, nuclear p65 was

increased in abundance for at least 60 min after stimulation, but in PKC η ^{-/-} T cells, the increase in the abundance of nuclear p65 ceased 20 min after stimulation (Fig. 5, G and H). The total amount of cellular p65 was not altered in PKC η ^{-/-} T cells (fig. S8C). Together, these results demonstrated that the NF- κ B pathway was disrupted in the absence of PKC η at least as much as in the absence of PKC θ . TCR-proximal signaling and MAPK signaling pathways were normal in PKC η ^{-/-} T cells (fig. S8, D and E). Collectively, these results showed that PKC η ^{-/-} T cells were defective for Ca²⁺ and NF- κ B signaling, which were also adversely affected in PKC θ ^{-/-} T cells.

DKO mice reveal isoform-specific and redundant roles for PKC η and PKC θ

The normal T cell development, but the defective Ca²⁺ and NF- κ B signaling pathways, seen in PKC η ^{-/-} and PKC θ ^{-/-} mice, prompted us to investigate possible redundancy between PKC η and PKC θ in T cell development and function. To do this, we bred *Prckc η* ^{-/-}, *Prckh*^{-/-} double knockout (DKO) mice. In the thymus, DKO mice had a more substantial reduction in the numbers of DN1 and DN4 thymocytes than were observed in either of the single knockout mice (Fig. 6, A and D). At the mature SP stage, although PKC θ ^{-/-} mice showed a mild defect in positive selection, the DKO mice had the most marked defect (Fig. 6, B and E). Thus, comparing the PKC θ ^{-/-} and DKO mice revealed a redundant role for PKC η in positive selection. This finding was confirmed when we analyzed the most mature population of cells in the thymus, the CD5^{hi}TCR^{hi} cells (Fig. 6C). No difference was noted between PKC η ^{-/-} and wild-type B6 mice, but the minor defect in thymocyte development in PKC θ ^{-/-} mice (21), was exacerbated by concomitant loss of PKC η (Fig. 6, C and F). Collectively, these findings demonstrated redundancy between PKC η and PKC θ ; PKC η could substitute for PKC θ during positive selection, as was initially suggested by the increased abundance of PKC η and its recruitment to the immunological synapse in PKC θ ^{-/-} thymocytes (Fig. 1).

We performed a comprehensive analysis of the lymph nodes and spleens of B6 mice and the various PKC knockout strains (fig. S9). Although redundancy between PKC η and PKC θ was apparent in thymocyte development, we observed an isoform-specific phenotype in mature T cells in the lymph nodes. For example, DKO mice and normal B6 mice had the same total number of T cells, as well as similar numbers of CD4⁺ and CD8⁺ T cell subsets. In contrast, PKC η ^{-/-} and PKC θ ^{-/-} mice had the highest and lowest number of these subsets, respectively (fig. S9B). More evidence supporting an isoform-specific role for PKC η in the biology of peripheral T cells came from analysis of the ratio of CD4⁺ to CD8⁺ cells in wild-type B6 mice and PKC-deficient strains of mice (fig. S9E). The CD4:CD8 T cell ratio was highest in PKC η ^{-/-} mice (lymph nodes: 1.69 ± 0.29; spleen: 2.39 ± 0.47) and lowest in PKC θ ^{-/-} mice (lymph nodes: 1.04 ± 0.12; spleen: 1.31 ± 0.21), with wild-type mice exhibiting intermediate ratios (lymph nodes: 1.44 ± 0.31; spleen: 1.87 ± 0.53). The biased CD4:CD8 ratios seen in single PKC knockout mice were “corrected” in DKO mice (lymph nodes: 1.53 ± 0.34; spleen: 1.88 ± 0.39). Together, these results strengthen the notion that PKC η and PKC θ have both redundant and isoform-specific roles in T cell development.

To determine whether the redundancy between PKC η and PKC θ was also manifested in T cell function, we measured the ability of T cells from the various PKC knockout mice to undergo homeostatic proliferation in vivo. T cell homeostatic proliferation occurs in response to a lymphopenic environment and is driven by TCR signaling (26). We sorted naïve T cells from wild-type (Thy1.1⁺) and the different PKC knockout mice (all Thy1.2⁺), mixed them at a 1:1 ratio, labeled them with CFSE, and injected them into sublethally irradiated recipient mice. One week later, we determined the CFSE staining of donor T cells by flow cytometry. We found that PKC η ^{-/-} CD8⁺ cells proliferated less well than did wild-type cells, with the most severe proliferation defect seen in DKO cells. PKC θ ^{-/-} cells

showed no noticeable defect in proliferation compared to that of wild-type cells (Fig. 7A). That the homeostatic proliferation of DKO T cells was not completely abolished and that PKC $\eta^{-/-}$, but not PKC $\theta^{-/-}$, CD8⁺ T cells had a noticeable proliferative defect was surprising. It was possible that the use of polyclonal donor T cells in these experiments obscured a defect in the PKC-deficient cells. Therefore, we repeated this experiment with MHC class I-restricted OT-I TCR transgenic T cells as the donor cells. The DKO cells proliferated very poorly compared to the wild-type cells in recipient mice (Fig. 7B, left). We also observed a proliferative defect in the PKC $\eta^{-/-}$ cells, but not in the PKC $\theta^{-/-}$ cells, consistent with the earlier experiments. We also analyzed the proportions of wild type and PKC-deficient donor cells present in the recipient mice after one week. Although all of the cell combinations started at a 1:1 ratio, the proliferation of DKO cells was clearly outpaced by that of wild-type T cells (Fig. 7B, right). PKC $\eta^{-/-}$ cells also represented a reduced proportion of the cell population after a week, but the proportion of PKC $\theta^{-/-}$ cells was similar to that of the wild-type cells. These changes matched the data from the CFSE-labeling experiments, demonstrating that PKC η , not PKC θ , played a major role in the homeostatic proliferation of CD8⁺ T cells. In addition to TCR signaling, cytokines such as IL-7 and IL-15 can also promote homeostatic proliferation; however, altered responsiveness to these cytokines during homeostatic proliferation seems unlikely in the case of PKC $\eta^{-/-}$ and DKO T cells, because the amounts of IL-7R α (CD127) and IL-15R (CD122) on the surface of these cells was comparable to those of wild-type T cells (fig. S10).

DISCUSSION

The finding that the abundance of PKC η mRNA was increased during the positive selection of thymocytes (6, 7) was surprising given the widely accepted importance of PKC θ in T cell biology, in particular that PKC θ is recruited to the central region of the immunological synapse (9, 10). PKC η was also recruited to the immunological synapse during thymocyte development and in mature T cells. PKC η formed a diffuse pattern at the immunological synapse, such that although PKC η and PKC θ were co-recruited to the immunological synapse, PKC θ is concentrated at the central synapse, PKC η was not. Such different localization patterns might lead to different functions. This suggestion is consistent with our data showing that T cell activation involving immunological synapse formation (antigen-specific proliferation in response to APCs) was more severely affected in cells lacking PKC η than were responses that did not involve an immunological synapse, such as stimulation with antibody against CD3 or with a combination of PMA and ionomycin.

Knockout mice have been powerful tools in immunological studies, as evidenced by the studies of PKC θ in T cell biology (14, 16). In contrast, studies on PKC η have lagged behind. The first study of a PKC η knockout mouse was published several years ago, but lacked any immunological analysis (8). Until now, there has been no follow-up study of this or any other PKC η knockout mouse. In Table 1, we summarize the similarities and differences between PKC $\eta^{-/-}$, PKC $\theta^{-/-}$, and the DKO mice based on this study and work from others (14, 16, 20, 21). That thymocyte development was normal in PKC $\eta^{-/-}$ mice was not unexpected. Initial reports on PKC $\theta^{-/-}$ mice did not identify any defects in thymocyte development despite showing severely impaired mature T cell function (14, 16); however, a study reexamining thymocyte development in PKC $\theta^{-/-}$ mice showed a rather mild deficiency (21), which is also in agreement with our observations here. Therefore, it is possible that the lack of obvious developmental or functional defects in any single PKC knockout mouse strain results from a redundancy between PKC isoforms, especially those members within the same subfamily. This is evidenced in our PKC $\eta^{-/-}$ PKC $\theta^{-/-}$ DKO mice, in which positive selection was more severely impaired than in either single knockout mouse.

Although redundancy between different PKC isoforms obscures some roles of individual PKC isoforms, we did find clear individual roles for PKC η in this study. For example, a reduced homeostatic proliferation of CD8⁺ T cells (either polyclonal or OT-I TCR transgenic T cells) was seen only in PKC η ^{-/-} cells, but not in PKC θ ^{-/-} cells. Also, PKC η ^{-/-} mice had a higher ratio of CD4⁺ T cells to CD8⁺ T cells than did wild-type mice, whereas PKC θ ^{-/-} mice had a lower ratio. Knockout of both PKC isoforms resulted in a CD4:CD8 T cell ratio that was similar to that of wild-type mice. Previous work has shown that the ratio of CD4⁺ to CD8⁺ T cells is influenced by a number of factors during development (28-30); however, the effect of PKC knockout that we observed appeared to occur post-thymically, because SP thymocytes from the knockout mice did not show altered ratios of CD4⁺ to CD8⁺ T cells. Together, these results demonstrate PKC η -specific roles in T cells.

The enlarged lymph nodes seen in PKC η ^{-/-} mice relative to those of wild-type mice were also noted in PKC δ ^{-/-} animals (31), but were not observed in PKC θ ^{-/-} mice (14, 16). In PKC δ ^{-/-} mice, lymphadenopathy was associated with increased numbers of B cells as well as a marked increase in the ratio of B cells to T cells (31). However, the situation in PKC η ^{-/-} mice was more complicated. In the lymph nodes, the relative proportions of B cells and T cells were barely different (~4% difference), and thus were unlikely to account for the substantially increased cell numbers (40 to 50%) in the lymph nodes of the PKC η ^{-/-} mice compared to those of normal mice. In contrast, in the spleens of PKC η ^{-/-} mice, the numbers of B cells and T cells were reduced compared to those in spleens from wild-type mice. We speculate that the differences in lymphocyte numbers between the lymph nodes and spleens of the PKC η ^{-/-} mice may reflect altered lymphocyte homing, homeostasis, or both, and are worth further investigation. We found that Ca²⁺ flux and NF- κ B translocation were impaired in PKC η ^{-/-} T cells, but that TCR-proximal tyrosine phosphorylation events and MAPK signaling pathways were intact. These signaling defects are similar to those of PKC θ ^{-/-} T cells. Unlike PKC θ , about which there are many in-depth studies on the molecular signaling machinery (15, 18-20), the investigation of PKC η is still at an early stage.

One puzzle raised in this and other studies is that there is an apparent discrepancy between the severe defect seen in PKC θ ^{-/-} T cells in studies in vitro and the mostly mild (if any) defect observed in studies in vivo. For example, the absence of PKC θ impairs the differentiation of T helper type 2 (T_H2) cells but not that of T_H1 cells, which results in reduced immune responses against *Leishmania major* (32). Similarly, PKC θ -deficiency results in impaired responses to *Listeria monocytogenes* infection (33), but not to impaired antiviral immune responses (34, 35). As we showed here, PKC θ ^{-/-} CD8⁺ T cells showed normal homeostatic proliferation, whereas this was impaired in PKC η ^{-/-} CD8⁺ T cells. Thus, the deficiencies seen in PKC η ^{-/-} T cells in vivo were more striking than those of PKC θ ^{-/-} T cells. It will be interesting to determine how PKC η ^{-/-} and DKO T cells behave in vivo in response to viral and bacterial infections.

We have demonstrated that PKC η has specific, as well as redundant (with PKC θ), functions in T cell biology, which are separated by developmental stage. Although redundant during T cell development, specific roles for PKC η in the responsiveness of CD8⁺ T cells were apparent in the periphery. Deficiencies in CD8⁺ T cell responses to pMHC may cause the increased CD4:CD8 T cell ratio in peripheral T cells that we observed in the PKC η ^{-/-} mice. In addition, PKC η was required to balance the distribution of lymphocytes between different lymphoid organs. Together, these factors point to the importance of PKC η in T cell biology.

MATERIALS AND METHODS

Mice

B6.PL-*Thy1a/CyJ* (Thy1.1⁺CD45.2⁺) and B6.SJL-*Ptprca Pepcb/BoyJ* (Thy1.2⁺CD45.1⁺) mice were purchased from Jackson Laboratories. C57BL/6 (Thy1.2⁺CD45.2⁺) mice were bred at The Scripps Research Institute (TSRI). OT-I and OT-I *Tap*^{-/-} animals were obtained from S. Jameson and K. Hogquist (University of Minnesota, Minneapolis, MN), and *Prkcq*^{-/-} mice (14) and OT-I *Prkcq*^{-/-} were provided by A. Altman (La Jolla Institute for Allergy and Immunology). *Prkch*^{-/-} mice were generated in this study. All experiments were performed in accordance with the guidelines of the Animal Care and Use Committee of TSRI.

Antibodies, cytokines, and reagents

Antibodies against CD3 (145-2C11), CD4 (RM4.4, RM4.5, GK1.5), CD8 α (53-6.7), CD25 (PC61.5), CD62L (MEL14), CD44 (IM7), V β 5 (MR9-6), V β 6 (RR4-7), V β 11 (CTVB11), and V β 12 (CTVB12b), were obtained from eBioscience, Biolegend, or BD Biosciences. Antibodies against phosphorylated ERK1/2 (T202/Y204, clone 197G2), phosphorylated p38 MAPK (Thr¹⁸⁰/Tyr¹⁸², clone 3DT), α -tubulin, and β -actin were from Cell Signaling Technology. Antibodies against p65, PKC η , and PKC θ were obtained from Santa Cruz Biotechnology. Recombinant IL-3, IL-6, and stem cell factor (SCF) were obtained from PeproTech. Granulocyte macrophage colony-stimulating factor (GM-CSF) was generated as described previously (36). Streptavidin was obtained from Jackson ImmunoResearch Laboratories. The GeneJammer transfection reagent was from Stratagene. The AmiconUltra centrifugal filter device (UFC810024) was obtained from Millipore. EasySep Mouse total T cell, CD4⁺, and CD8⁺ T Cell Negative Enrichment Kits were from StemCell Technologies. Indo-1 AM and CFDA-SE (CFSE) were from Molecular Probes (Invitrogen).

Real time RT-PCR

Total RNA from the thymi of 4- to 8-week old OT-I mice or from sorted subpopulations was isolated with the RNeasy Mini Kit (Qiagen). The RNA was treated with deoxyribonuclease I (DNase I, Invitrogen) for 15 min at room temperature. The reaction was stopped by the addition of 25 mM EDTA, and the DNase was inactivated by incubating the samples at 65°C for 10 min. RNA samples were used as templates to synthesize complementary DNA (cDNA) with the Superscript First Strand Synthesis System for RT-PCR (Invitrogen) according to the manufacturer's recommendations. Oligonucleotide primers were designed with Primer Express 1.5 software (PE Applied Biosystems). The primer sequences are as follows: PKC η 5' primer: 5'-CTCCAGACCGTCTGTTCTTTGTC-3'; 3' primer: 5'-ATCTCCGCGGCGTAGAAA-3', GenBank accession # D90242. Ribosomal protein 5' primer: 5'-AGATGCAGCAGATCCGCAT-3'; 3' primer: 5'-GGATGGCCTTGCGCA-3', GenBank accession # BC011106. Real-time PCR reactions were performed on the ABI Prism 7700 Sequence Detection System with SYBR Green PCR Master Mix (PE Applied Biosystems). The PCR mix was optimized for SYBR Green reactions and contained SYBR Green 1 dye, AmpliTaqGold DNA polymerase, and dNTPs with dUTP. Each reaction was performed in a final volume of 25 μ l and contained the SYBR Green PCR Master Mix, cDNA, and 150 nM of each primer. Two independent experiments were performed, and all reactions were performed in duplicate. A standard curve with a two-fold serial dilution of the standard cDNA was generated for the target gene as well as for the housekeeping gene ribosomal protein. cDNAs (20 ng/reaction) from the different cell populations were used as templates for real-time PCR. The standard curves were used to determine the relative concentrations of amplified transcripts. The amounts of PKC η mRNA were first normalized to those of the ribosomal protein mRNA. The normalized sample values were finally divided

by the normalized amounts of PKC η mRNA in samples from OT-I TCR^{lo} DP cells to obtain the fold-change in mRNA abundance between the different populations of DP thymocytes.

Generation of PKC η ^{-/-} mice

The strategy for generating PKC η knockout mice was as described previously (fig. S5) (37), except that all cloning materials, embryonic stem (ES) cell line (Bruce4), and founder mice used for breeding were on a B6 background. PKC θ knockout mice were described previously (14) and were maintained in TSRI animal facility by further breeding onto the B6 background. DKO mice were generated by breeding PKC η ^{-/-} and PKC θ ^{-/-} mice together.

T cell activation and proliferation assays

Purified naïve CD8⁺ T cells from mice were used in experiments as indicated in the text. Purification was performed with biotinylated antibodies in conjunction with magnetic beads conjugated with antibodies against biotin (BD Bioscience) or else cells were sorted with a flow cytometer. Cells were stimulated with plate-bound or soluble antibody against CD3 as indicated in the figures, and cells were incubated with antibodies against CD69, CD25, CD4, and CD8 for flow cytometric analysis. Thymidine incorporation assays were performed as described (14). For proliferation assays involving CFSE dilution, lymphocytes were incubated with CFSE (0.2 μ M) at 37°C for 10 min, which was stopped by the addition of 10 volumes of cRPMI. After washing, cells were cultured with or without antibody against CD3 in cRPMI for 48 hours, or in the presence of irradiated B6.SJL-*Ptprca Pepcb/BoyJ* (CD45.1) splenocytes that had been pulsed with the indicated concentration of OVA peptide. T cell proliferation was determined by measuring the dilution of CFSE in cells by flow cytometry. To measure IL-2 production, CD4⁺ T cells were purified from lymph nodes with the EasySep Mouse CD4⁺ T Cell Enrichment Kit (StemCell), and 2×10^5 cells were seeded per well in a BioCoat T-Cell Activation Plate, which was pre-coated with antibody against CD3 (BD Biosciences). To stimulate cells, soluble antibody against CD28 was added to the cell culture medium to a final concentration of 1 μ g/ml, and cells were incubated at 37°C in 5% CO₂ for 48 hours. Culture supernatants were removed, and the concentration of IL-2 produced by the cells was measured with the mouse IL-2 enzyme-linked immunosorbent assay (ELISA) Ready-SET-Go kit (eBioscience) according to the manufacturer's instructions.

Ca²⁺ signaling

Ca²⁺ flux was performed as described previously (37, 38). Briefly, lymphocytes were isolated from wild-type mice (Thy1.1⁺ or Thy1.2⁺) and PKC η ^{-/-} mice (Thy1.2⁺). Cells from different genotypes were mixed at a 1:1 ratio. Cells were suspended at 2 to 5×10^6 /ml in cRPMI [RPMI medium supplemented with 10% fetal calf serum (FCS), penicillin (100 U/ml), streptomycin (10 μ g/ml), glutamine (292 μ g/ml), 50 μ M 2-mercaptoethanol, and 25 mM Hepes (pH 7.2-7.5)] and were incubated with 2 μ M Indo-1 AM for 30 min at 37°C in 5% CO₂. Cells were washed twice with cRPMI and resuspended in 0.5 ml of cRPMI or cHBSS [Hanks' balanced salt solution (HBSS) supplemented with 1% FCS, 1 mM EGTA, 1 mM MgCl₂, and 10 mM Hepes (pH 7.2-7.5)]. Cells were pre-warmed to 37°C before analysis and were kept at 37°C during event collection on a Becton-Dickinson LSR-II flow cytometer. To stimulate cells, reagents were added during the analysis as indicated in the figures, and maximal Ca²⁺ flux was obtained by adding ionomycin (500 ng/ml, Calbiochem). The mean fluorescence ratio was calculated with FlowJo software (TreeStar).

Western blotting analysis

CD8⁺ T cells were stimulated with crosslinking antibodies against CD3 and CD8 for the times indicated in the figures. Cell lysates were prepared, resolved by SDS-polyacrylamide

gel electrophoresis (SDS-PAGE), and analyzed by Western blotting with the indicated antibodies, as described previously (37). To measure the nuclear translocation of NF- κ B p65, cells were stimulated as described earlier, chilled on ice, and fractionated with the NE-PER kit (Pierce). Western blotting analysis of samples was performed with the Li-Cor Odyssey infrared imaging system. Normalization and calculation of fraction purity and the ratios of nuclear to cytosolic p65 abundance were performed according to Li-Cor protocols with p65, total protein, actin, and tubulin signals.

In vivo proliferation assays

Proliferation of OT-I TCR transgenic cells in response to stimulation with OVA peptide in vivo was measured as described previously (39). Briefly, OT-I TCR CD8⁺ T cells were purified with a CD8⁺ T cell Negative Enrichment kit (StemCell). Wild-type (Thy1.1⁺CD45.2⁺) and PKC $\eta^{-/-}$ (Thy1.2⁺CD45.2⁺) cells were mixed at a 1:1 ratio, and transferred into recipient B6.SJL mice (Thy1.2⁺CD45.1⁺). The recipient mice were intravenously injected with BMDCs that had been pulsed with OVA₂₅₇₋₂₆₄ peptide one day before transfer of the T cells. At various time points, cells from the lymph nodes and spleens of recipient mice were collected, and the proportions and absolute cell numbers of donor cells were determined by flow cytometry. BMDC were cultured and induced to maturation as described previously (36, 39, 40). Briefly, on day 7 of BMDC culture, lipopolysaccharide (LPS, 100 ng/ml) was added overnight to induce maturation. BMDC maturity and phenotype were confirmed by flow cytometric analysis of the surface expression of CD11c, CD86, CD80, and MHC-II. The resultant cell population contained >90% CD11c⁺ MHC-II^{hi} BMDCs.

Homeostatic proliferation assays

Naïve T cells (CD62L⁺CD44⁻) were sorted from mice (all of whom were CD45.2⁺, but were either Thy1.1⁺ or Thy1.2⁺). Thy1.1⁺ or Thy1.2⁺ sorted cells were mixed in a 1:1 ratio, labeled with CFSE, and injected intravenously into recipient B6.SJL mice (Thy1.2⁺CD45.1⁺), which were sublethally irradiated (5.5 Gy) with a Gammacell 40 (MDS Nordion) before cell transfer. One week later, cells from the lymph nodes and spleens of recipient mice were collected and analyzed by flow cytometry.

Microscopy

To visualize the recruitment of PKC to the immunological synapse in live cells, we transfected T cell hybridomas with plasmid encoding fusion proteins of PKC isoforms and fluorescent proteins, as indicated in the text. The form of red fluorescent protein (RFP) used was tDimer2(12) (41). APCs were loaded with peptides or superantigens as indicated in the figures. T cell hybridomas and APCs were mixed together for various time points and were fixed before imaging. For time-lapse imaging of T cell-APC conjugates (fig. S4), T cell hybridomas and APCs were sequentially loaded into an FCS2 flow chamber FCS2 (Bioptechs) that was heated to 37°C. To visualize the recruitment of PKC to the immunological synapse in live primary T cells, we incubated 1×10^7 thymocytes with 2×10^7 EL4 cells that were pulsed with OVA peptide (10 mM) or with 2×10^7 LK35 B cell (class II⁺) tumor cells presenting the superantigens SEA (50 ng/ml) and SEB (10 μ g/ml, Toxin Technology) in 96-well, round-bottomed plates for 30 or 60 min at 37°C. Thymocytes were then fixed with 4% paraformaldehyde (PFA) for 12 min at room temperature. To detect cell-surface markers, thymocytes were incubated with biotinylated antibodies against CD4, CD8, or LFA-1 (BD Bioscience), after which they were incubated with Alexa Fluor 488-conjugated streptavidin (Molecular Probes). For intracellular staining, cells were permeabilized with 0.2% saponin for 15 min at room temperature. Cells were then incubated with rabbit antibodies against the appropriate PKC isoform, after which they were incubated with Alexa Fluor 568- or Alexa Fluor 680-conjugated antibodies against rabbit antibodies

(Molecular Probes). To visualize the nuclear translocation of NF- κ B in primary T cells, we purified 2×10^6 CD8⁺ T cells from lymph nodes by magnetic negative selection and plated the cells on Lab-Tek II chambered cover glass coated with poly-D-lysine (Sigma). The cells were then stimulated with crosslinking antibodies against CD3 and CD8 for the times indicated in the figures. T cells were then fixed with 4% PFA for 12 min at room temperature. Cells were permeabilized with 0.3% Triton X-100 for 3 min at room temperature. Cells were then incubated with rabbit antibody against p65 (1 μ g/ml), after which they were incubated with Alexa Fluor 488-conjugated secondary antibody against rabbit antibody (Molecular Probes). Nuclei were counterstained with the DNA-binding dye 4',6-diamidino-2-phenylindole (DAPI; Invitrogen). All images were captured with a Zeiss Axiovert 200 M inverted microscope. SlideBook software (Intelligent Imaging Innovation) was used for the capture as well as for deconvolution and image analysis, and ImageJ was used for image presentation.

Statistical analysis

Statistical differences were calculated with the mean difference hypothesis of Student's two tailed *t* test assuming different variances and a confidence level of 95%. Calculations were performed with Microsoft Excel.

Supplementary Material

Refer to Web version on PubMed Central for supplementary material.

Acknowledgments

We thank A. Altman (La Jolla Institute for Allergy and Immunology), K. Hogquist and S. Jameson (University of Minnesota, Minneapolis), and D. Littman (Skirball Institute, New York) for mice and reagents, and the TSRI Mouse Genetics Core for help in making the knockout mice.

Funding: This work was supported by grants from NIH (GM048002 and GM065230 to N.R.J.G., OD006433 to H.C., and AI070845 to K.S.). N.N.-M. was supported by a fellowship from the Swiss National Science Foundation; J.C. was supported by a fellowship from the Spanish Ministerio de Innovacion y Ciencia (MICIN); P.P.Y. was supported by NIH training grant T32HL07195; J.A.H.H. was supported by the Irving S. Sigal Fellowship of the American Chemical Society and by NIH training grant T32AI07244; and K.S. was supported by The Leukemia & Lymphoma Society Scholar Award 1440-11. The content of this work is solely the responsibility of the authors and does not necessarily represent the official views of the National Institute of General Medicine or the National Institutes of Health. This is manuscript number 20858 from The Scripps Research Institute.

REFERENCES AND NOTES

1. Dempsey EC, Newton AC, Mochly-Rosen D, Fields AP, Reyland ME, Insel PA, Messing RO. Protein kinase C isozymes and the regulation of diverse cell responses. *Am J Physiol Lung Cell Mol Physiol.* 2000; 279:L429–438. [PubMed: 10956616]
2. Isakov N, Altman A. Protein kinase C θ in T cell activation. *Annu Rev Immunol.* 2002; 20:761–794. [PubMed: 11861617]
3. Baier G. The PKC gene module: molecular biosystematics to resolve its T cell functions. *Immunol Rev.* 2003; 192:64–79. [PubMed: 12670396]
4. Hayashi K, Altman A. Protein kinase C θ (PKC θ): a key player in T cell life and death. *Pharmacol Res.* 2007; 55:537–544. [PubMed: 17544292]
5. Manicassamy S, Gupta S, Sun Z. Selective function of PKC- θ in T cells. *Cell Mol Immunol.* 2006; 3:263–270. [PubMed: 16978534]
6. Mick VE, Starr TK, McCaughy TM, McNeil LK, Hogquist KA. The regulated expression of a diverse set of genes during thymocyte positive selection *in vivo*. *J Immunol.* 2004; 173:5434–5444. [PubMed: 15494490]

7. Niederberger N, Buehler LK, Ampudia J, Gascoigne NRJ. Thymocyte stimulation by anti-TCR- β , but not by anti-TCR- α , leads to induction of developmental transcription program. *J Leukoc Biol.* 2005; 77:830–841. [PubMed: 15661827]
8. Chida K, Hara T, Hirai T, Konishi C, Nakamura K, Nakao K, Aiba A, Katsuki M, Kuroki T. Disruption of protein kinase C η results in impairment of wound healing and enhancement of tumor formation in mouse skin carcinogenesis. *Cancer Res.* 2003; 63:2404–2408. [PubMed: 12750259]
9. Monks CRF, Kupfer H, Tamir I, Barlow A, Kupfer A. Selective modulation of protein kinase C- θ during T-cell activation. *Nature.* 1997; 385:83–86. [PubMed: 8985252]
10. Monks CRF, Freiberg BA, Kupfer H, Sciaky N, Kupfer A. Three-dimensional segregation of supramolecular activation clusters in T cells. *Nature.* 1998; 395:82–86. [PubMed: 9738502]
11. Grakoui A, Bromley SK, Sumen C, Davis MM, Shaw AS, Allen PM, Dustin ML. The immunological synapse: a molecular machine controlling T cell activation. *Science.* 1999; 285:221–227. [PubMed: 10398592]
12. Yokosuka T, Kobayashi W, Sakata-Sogawa K, Takamatsu M, Hashimoto-Tane A, Dustin ML, Tokunaga M, Saito T. Spatiotemporal regulation of T cell costimulation by TCR-CD28 microclusters and protein kinase C θ translocation. *Immunity.* 2008; 29:589–601. [PubMed: 18848472]
13. Singleton KL, Roybal KT, Sun Y, Fu G, Gascoigne NRJ, van Oers NS, Wulfiging C. Spatiotemporal patterning during T cell activation is highly diverse. *Sci Signal.* 2009; 2:ra15. [PubMed: 19351954]
14. Sun Z, Arendt CW, Ellmeier W, Schaeffer EM, Sunshine MJ, Gandhi L, Annes J, Petrzilka D, Kupfer A, Schwartzberg PL, Littman DR. PKC- θ is required for TCR-induced NF- κ B activation in mature but not immature T lymphocytes. *Nature.* 2000; 404:402–407. [PubMed: 10746729]
15. Egawa T, Albrecht B, Favier B, Sunshine MJ, Mirchandani K, O'Brien W, Thome M, Littman DR. Requirement for CARMA1 in antigen receptor-induced NF- κ B activation and lymphocyte proliferation. *Curr Biol.* 2003; 13:1252–1258. [PubMed: 12867038]
16. Pfeifhofer C, Kofler K, Gruber T, Tabrizi NG, Lutz C, Maly K, Leitges M, Baier G. Protein kinase C θ affects Ca²⁺ mobilization and NFAT cell activation in primary mouse T cells. *J Exp Med.* 2003; 197:1525–1535. [PubMed: 12782715]
17. Hara H, Bakal C, Wada T, Bouchard D, Rottapel R, Saito T, Penninger JM. The molecular adapter Carma1 controls entry of I κ B kinase into the central immune synapse. *J Exp Med.* 2004; 200:1167–1177. [PubMed: 15520247]
18. Wang D, Matsumoto R, You Y, Che T, Lin XY, Gaffen SL, Lin X. CD3/CD28 costimulation-induced NF- κ B activation is mediated by recruitment of protein kinase C- θ , Bcl10, and I κ B kinase β to the immunological synapse through CARMA1. *Mol Cell Biol.* 2004; 24:164–171. [PubMed: 14673152]
19. Roose JP, Mollenauer M, Gupta VA, Stone J, Weiss A. A diacylglycerol-protein kinase C-RasGRP1 pathway directs Ras activation upon antigen receptor stimulation of T cells. *Mol Cell Biol.* 2005; 25:4426–4441. [PubMed: 15899849]
20. Manicassamy S, Sadim M, Ye RD, Sun Z. Differential roles of PKC- θ in the regulation of intracellular calcium concentration in primary T cells. *J Mol Biol.* 2006; 355:347–359. [PubMed: 16309697]
21. Morley SC, Weber KS, Kao H, Allen PM. Protein kinase C- θ is required for efficient positive selection. *J Immunol.* 2008; 181:4696–4708. [PubMed: 18802072]
22. Irwin MJ, Gascoigne NRJ. Interplay between superantigens and the immune system. *J. Leukocyte Biol.* 1993; 54:495–503. [PubMed: 8228628]
23. Yachi PP, Ampudia J, Gascoigne NRJ, Zal T. Nonstimulatory peptides contribute to antigen-induced CD8-T cell receptor interaction at the immunological synapse. *Nat Immunol.* 2005; 6:785–792. [PubMed: 15980863]
24. Starr TK, Jameson SC, Hogquist KA. Positive and negative selection of T cells. *Annu Rev Immunol.* 2003; 21:139–176. [PubMed: 12414722]
25. Scherer MT, Ignatowicz L, Winslow GM, Kappler JW, Marrack P. Superantigens: Bacterial and viral proteins that manipulate the immune system. *Annu. Rev. Cell Biol.* 1993; 9:101–128. [PubMed: 7506550]

26. Sprent J, Surh CD. Normal T cell homeostasis: the conversion of naive cells into memory-phenotype cells. *Nat Immunol.* 2011; 12:478–484. [PubMed: 21739670]
27. Liu KQ, Bunnell SC, Gurniak CB, Berg LJ. T cell receptor-initiated calcium release is uncoupled from capacitative calcium entry in Itk-deficient T cells. *J. Exp. Med.* 1998; 187:1721–1727. [PubMed: 9584150]
28. Suzuki H, Punt JA, Granger LG, Singer A. Asymmetric signaling requirements for thymocyte commitment to the CD4+ versus CD8+ T cell lineages: a new perspective on thymic commitment and selection. *Immunity.* 1995; 2:413–425. [PubMed: 7719943]
29. Corbella P, Moskophidis D, Spanopoulou E, Mamalaki C, Tolaini M, Itano A, Lans D, Baltimore D, Robey E, Kioussis D. Functional commitment to helper T cell lineage precedes positive selection and is independent of T cell receptor MHC specificity. *Immunity.* 1994; 1:269–276. [PubMed: 7889414]
30. Sim B-C, Aftahi N, Reilly C, Bogen B, Schwartz RH, Gascoigne NRJ, Lo D. Thymic skewing of the CD4/CD8 ratio maps with the T-cell receptor α -chain locus. *Curr. Biol.* 1998; 8:701–704. [PubMed: 9637921]
31. Mecklenbrauker I, Saijo K, Zheng NY, Leitges M, Tarakhovsky A. Protein kinase C δ controls self-antigen-induced B-cell tolerance. *Nature.* 2002; 416:860–865. [PubMed: 11976686]
32. Marsland BJ, Soos TJ, Spath G, Littman DR, Kopf M. Protein kinase C θ is critical for the development of in vivo T helper (Th)2 cell but not Th1 cell responses. *J Exp Med.* 2004; 200:181–189. [PubMed: 15263025]
33. Sakowicz-Burkiewicz M, Nishanth G, Helmuth U, Drogemuller K, Busch DH, Utermohlen O, Naumann M, Deckert M, Schluter D. Protein kinase C- θ critically regulates the proliferation and survival of pathogen-specific T cells in murine listeriosis. *J Immunol.* 2008; 180:5601–5612. [PubMed: 18390745]
34. Berg-Brown NN, Gronski MA, Jones RG, Elford AR, Deenick EK, Odermatt B, Littman DR, Ohashi PS. PKC θ signals activation versus tolerance in vivo. *J Exp Med.* 2004; 199:743–752. [PubMed: 15024044]
35. Marsland BJ, Nembrini C, Schmitz N, Abel B, Krautwald S, Bachmann MF, Kopf M. Innate signals compensate for the absence of PKC- θ during in vivo CD8⁺ T cell effector and memory responses. *Proc Natl Acad Sci U S A.* 2005; 102:14374–14379. [PubMed: 16186501]
36. Fu G, Wijburg OL, Cameron PU, Price JD, Strugnell RA. Salmonella enterica Serovar Typhimurium infection of dendritic cells leads to functionally increased expression of the macrophage-derived chemokine. *Infect Immun.* 2005; 73:1714–1722. [PubMed: 15731072]
37. Fu G, Vallee S, Rybakina V, McGuire MV, Ampudia J, Brockmeyer C, Salek M, Fallen PR, Hoerter JAH, Munshi A, Huang YH, Hu J, Fox HS, Sauer K, Acuto O, Gascoigne NRJ. Themis controls thymocyte selection through regulation of T cell antigen receptor-mediated signaling. *Nat Immunol.* 2009; 10:848–856. [PubMed: 19597499]
38. Fu G, Gascoigne NRJ. Multiplexed labeling of samples with cell tracking dyes facilitates rapid and accurate internally controlled calcium flux measurement by flow cytometry. *J Immunol Methods.* 2009; 350:194–199. [PubMed: 19647745]
39. Krieg C, Boyman O, Fu YX, Kaye J. B and T lymphocyte attenuator regulates CD8+ T cell-intrinsic homeostasis and memory cell generation. *Nat Immunol.* 2007; 8:162–171. [PubMed: 17206146]
40. Lutz MB, Kukutsch N, Ogilvie AL, Rossner S, Koch F, Romani N, Schuler G. An advanced culture method for generating large quantities of highly pure dendritic cells from mouse bone marrow. *J Immunol Methods.* 1999; 223:77–92. [PubMed: 10037236]
41. Campbell RE, Tour O, Palmer AE, Steinbach PA, Baird GS, Zacharias DA, Tsien RY. A monomeric red fluorescent protein. *Proc. Natl. Acad. Sci. USA.* 2002; 99:7877–7882. [PubMed: 12060735]

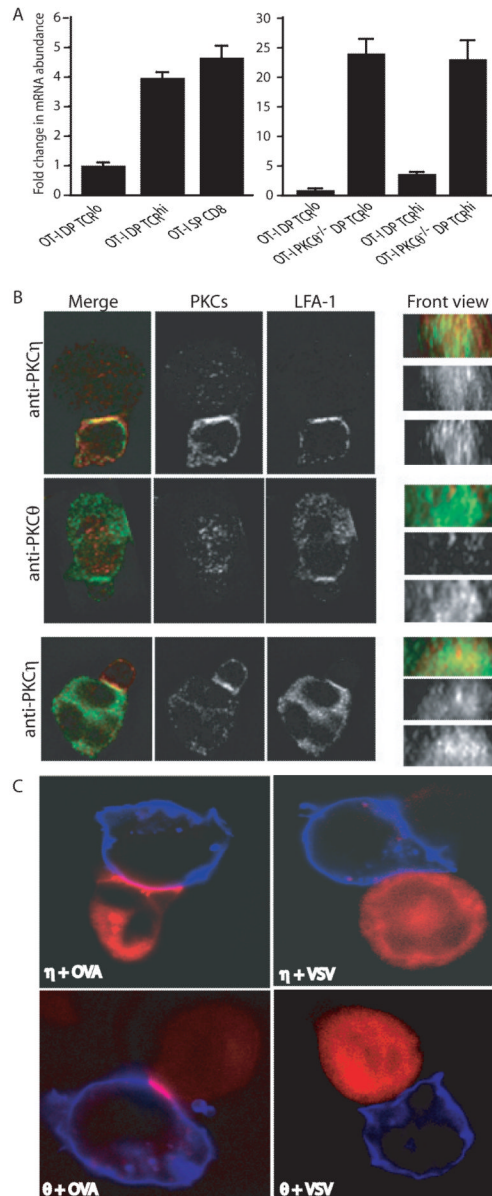


Fig. 1. Analysis of PKC η abundance and localization. **(A)** PKC η mRNA is increased in abundance during positive selection. PKC η mRNA abundance was determined by real-time RT-PCR. Results are shown as fold change compared to the amount of PKC η mRNA in OT-I TCR^{lo} cells. Data are representative of two experiments, each performed in duplicate. **(B)** PKC η recruitment to the immunological synapse in the absence of PKC θ . To avoid potential cross reactivity of PKC-specific antibodies, we used thymocytes and mature T cells from PKC $\theta^{-/-}$ mice. After activation with superantigen-loaded LK35 cells, T cells or thymocytes were incubated with antibodies against LFA-1 and the PKC isoforms (anti-PKC θ and anti-PKC η), after which they were incubated with antisera against rabbit immunoglobulin (Ig). In the merged image panel, LFA-1 staining is shown in green, whereas PKC staining is in red. The larger cells are LK35 cells and the smaller cells are T cells. Top and middle panels show thymocytes and the bottom panels show mature T cells, with corresponding en face views shown on the right. Data are representative of at least 50 cell-cell conjugates of each

type. (C) Recruitment of PKC η to the immunological synapse in live cells. OT-I T hybridomas transfected with plasmid encoding PKC η -RFP (η) or PKC θ -RFP (θ) were stimulated with EL4 cells that were pulsed with OVA or VSV peptides. PKC protein is shown in red, whereas EL4 cells are shown in blue. Images are representative of at least 20 cells collected from three experiments.

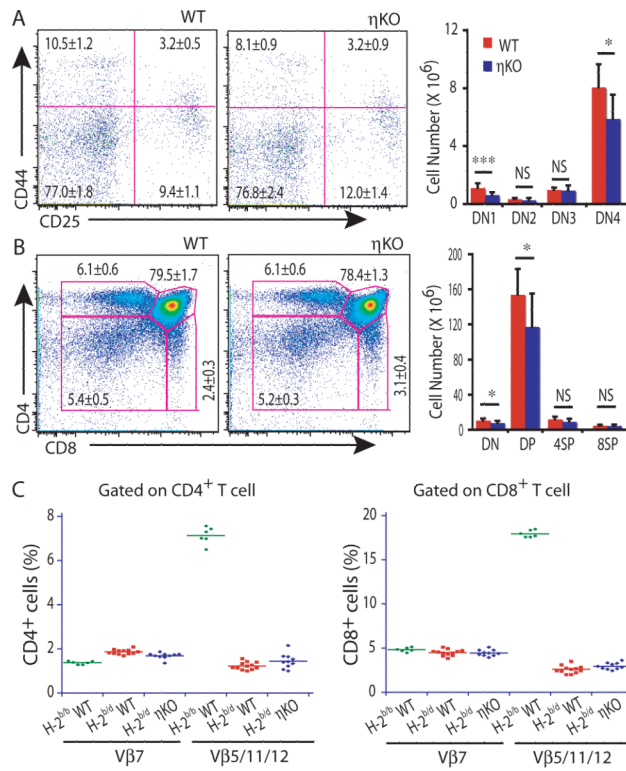


Fig. 2. Thymocyte development in $PKC\eta^{-/-}$ mice is normal. Thymocytes from age- and sex-matched wild-type (WT) ($n = 8$ mice) and $PKC\eta^{-/-}$ mice (ηKO , $n = 8$ mice) were analyzed for the presence of (A) $CD4^{-}CD8^{-}$ (DN) subsets, (B) $CD4^{+}$ and $CD8^{+}$ (DP, SP) and DN subsets. Left: representative flow cytometry plots showing the mean percentages of each subset \pm the standard deviation (SD). Right: mean total numbers of cells \pm SD for each subset. P values were calculated by Student's t test. $*P \leq 0.05$; $***P \leq 0.001$. (C) Negative selection of $PKC\eta^{-/-}$ thymocytes is normal. T cells expressing $V\beta 5$, $V\beta 11$, or $V\beta 12$, but not $V\beta 7$, were deleted by endogenous mouse mammary tumor virus-encoded superantigens in mice that express I-E ($H-2^{b/d}$) but not in mice lacking I-E ($H-2^{b/b}$). $PKC\eta^{-/-}$ thymocytes bearing $V\beta 5$, $V\beta 11$, or $V\beta 12$ were deleted similarly to wild-type thymocytes. Each dot represents a single mouse.

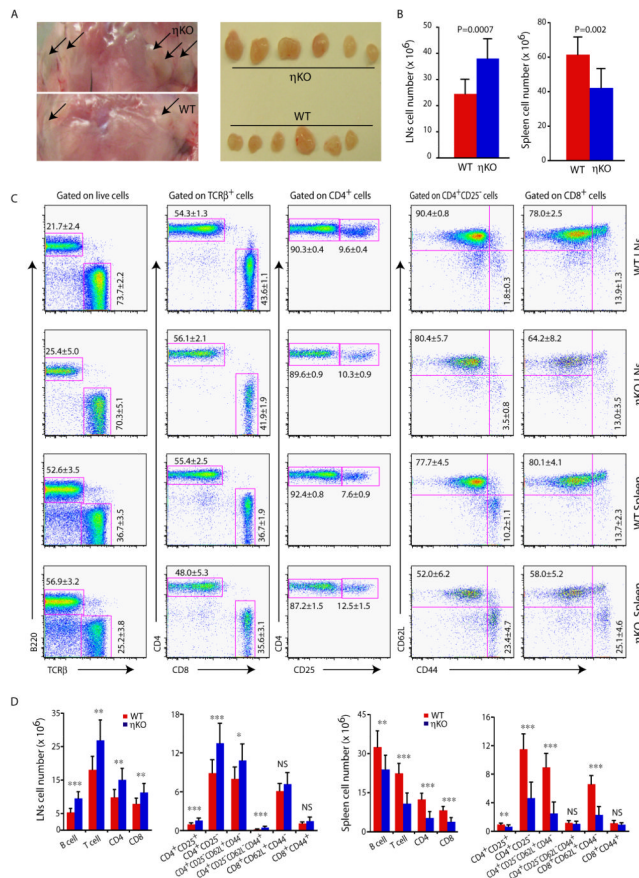


Fig. 3. PKC $\eta^{-/-}$ mice have enlarged lymph nodes. The mice analyzed in Fig. 2 were examined to determine the phenotype of their peripheral T cells. **(A)** Lymph nodes from the cervical area were photographed and are shown on the left; arrows indicate readily identifiable lymph nodes. On the right are axillar, brachial, and inguinal lymph nodes that were isolated from mice and aligned for comparison. **(B)** Total lymphocyte numbers from six pooled axillar, brachial, and inguinal lymph nodes are shown on the left, whereas total lymphocyte numbers from spleens are shown on the right. **(C)** Representative flow cytometry plots of lymph nodes (LNs) and spleens are shown with the proportion of each cell type listed as the mean \pm SD. **(D)** Absolute cell numbers of the indicated subsets are listed for lymph nodes and spleen. For cell numbers, P values calculated by Student's t test are shown as: * $P \leq 0.05$; ** $P \leq 0.01$; *** $P \leq 0.001$; NS, not significant, $n=8$ mice. Representative of 3 experiments.

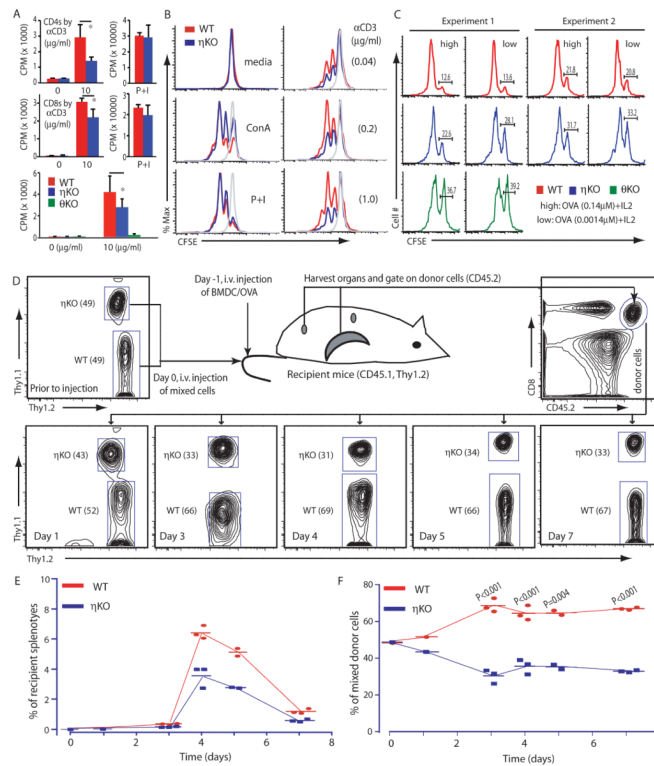


Fig. 4. Proliferation of PKC $\eta^{-/-}$ mature T cells is impaired. (A) Naïve T cells were stimulated with antibody against CD3 or with PMA and ionomycin (P+I) for 64 hours, and 3 H-thymidine was added to the culture medium for the last 16 hours. Graph shows proliferation as mean counts per minute (CPM) of 3 H incorporated into DNA \pm SD of replicates ($n \geq 3$). (B) Lymph node cells from WT (CD45.1 $^{+}$) and PKC η KO (CD45.2 $^{+}$) mice were mixed, labeled with CFSE, and stimulated as indicated for 48 hours. Dilution of CFSE was analyzed by flow cytometry after gating for CD45 allotype and CD8. (C) OTI TCR Tg WT (CD45.2 $^{+}$ Thy1.1 $^{+}$) and PKC $\eta^{-/-}$ or PKC $\theta^{-/-}$ (both CD45.2 $^{+}$ Thy1.2 $^{+}$) naïve T cells were purified, mixed in a 1:1 ratio, labeled with CFSE, and stimulated with irradiated splenocytes (CD45.1 $^{+}$) that were pulsed with OVA peptide. After 48 hours, CFSE dilution was analyzed by flow cytometry. The percentages of undivided cells are indicated for two independent experiments. (D) Antigen-specific proliferation of PKC $\eta^{-/-}$ T cells is impaired in vivo. Experiments were designed as depicted in the cartoon. Flow cytometry plots show the proportions of WT and KO donor cells that were present at the indicated times. (E) Proportions of WT and PKC η KO donor cells per recipient mouse spleen. (F) Proportions of WT and PKC η KO cells within donor cell population. Each dot in (E) and (F) represents an individual mouse. * $P \leq 0.05$. Data are representative of three (A) or four (B) and (D to F) independent experiments.

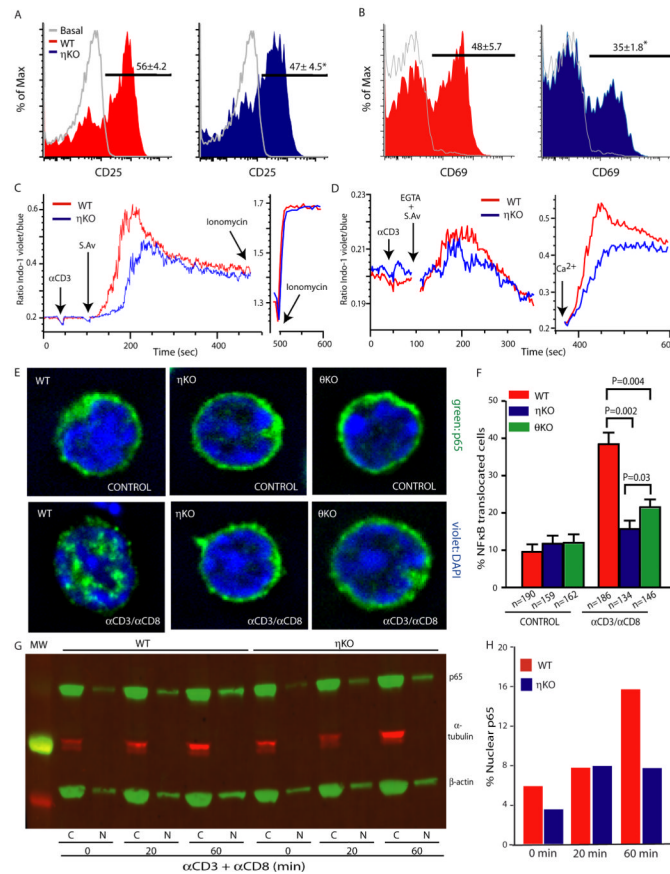


Fig. 5. Impaired signaling in mature PKC $\eta^{-/-}$ T cells. (**A**, **B**) Increased abundance of activation markers. Lymph node cells were activated by stimulation with antibody against CD3 for 16 hours, and the surface abundance of (**A**) CD25 and (**B**) CD69 was analyzed on CD8⁺ cells by flow cytometry. The gray line indicates the basal abundance of these markers on nonstimulated cells, whereas the color-hatched region represents stimulated cells. CD25⁺ and CD69⁺ cell populations are marked and the mean percentages \pm SD are shown. The asterisk indicates statistically significant difference (by *t* test) between KO and WT mice ($n = 3$ mice); $P = 0.05$ for CD25 and $P < 0.05$ for CD69. (**C** and **D**) Analysis of Ca²⁺ signaling. Cells from WT (Thy1.1⁺) and PKC η KO (Thy1.2⁺) mice were mixed, loaded with Indo-1, and stimulated by crosslinking biotinylated antibody against CD3 (α CD3) with streptavidin (S.Av). Ca²⁺ flux was recorded by flow cytometry. (**E** and **F**) Imaging of the nuclear translocation of NF- κ B p65 protein. Purified CD8⁺ T cells were stimulated with antibodies against CD3 (α CD3) and CD8 (α CD8) for 60 min, and the nuclear translocation of p65 was determined by microscopy as shown in (**E**), and summarized in (**F**). (**G** and **H**) Examination of the nuclear translocation of p65 by Western blotting analysis. Cells were stimulated as shown in (**E** and **F**), after which, cytosolic and nuclear extracts were prepared and subjected to Western blotting analysis (**G**). Normalized data are shown (**H**). Data are representative of two (**A**, **B**, **G**, and **H**) or 4 (**C** to **F**) experiments.

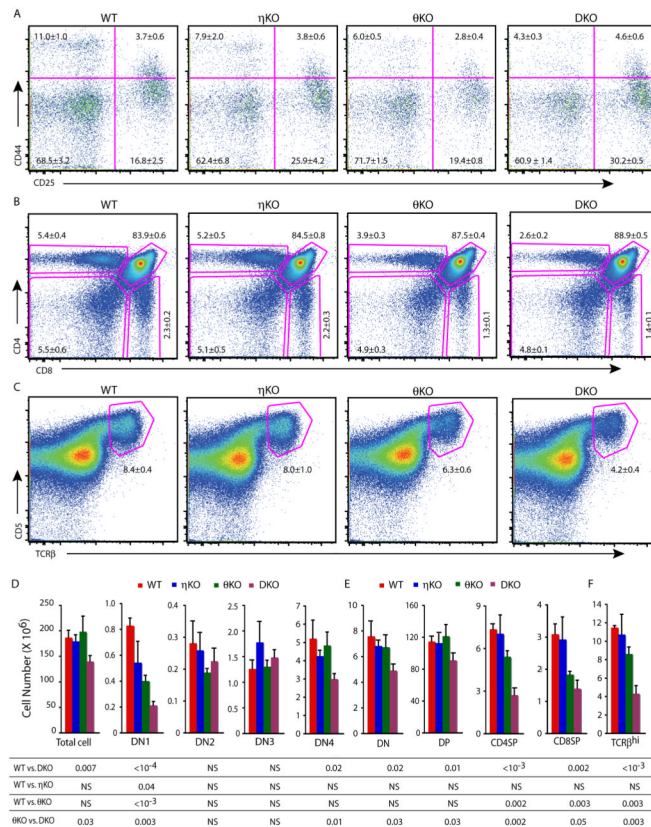
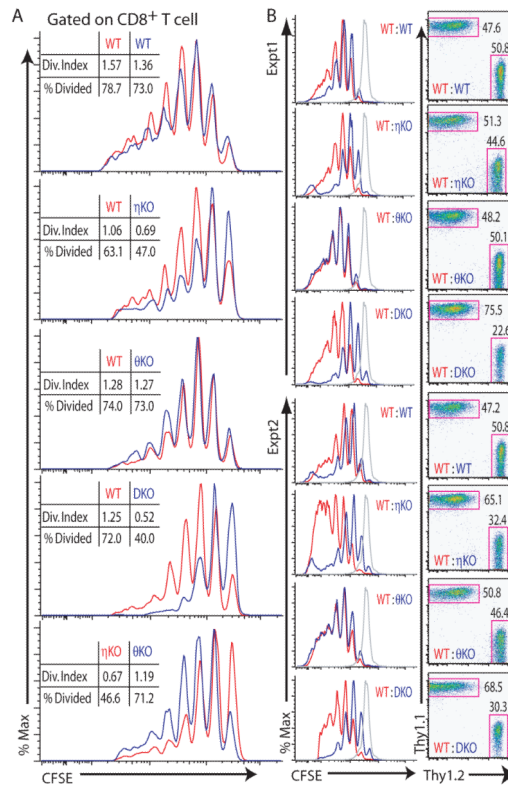


Fig. 6. Comparison of thymic phenotypes in three PKC-deficient mouse strains. Three age- and sex-matched mice from each genotype were used in this analysis. Representative flow cytometry plots of (A) DN1 to DN4 stage thymocytes, (B) DN, DP, and SP stage thymocytes, and (C) the most mature CD5^{hi}TCR^{hi} thymocytes are shown with the proportions of each cell type listed as mean ± SD. Absolute cell numbers for each subset are listed in (D), (E), and (F) respectively. *P* values were calculated with the Student's *t* test and are listed underneath as indicated. Data are representative of three experiments.

**Fig. 7.**

Comparison of homeostatic proliferation in three PKC-deficient mouse strains. Homeostatic proliferation assays were performed with (A) naïve polyclonal T cells or (B) naïve OT-I TCR Tg T cells as donor cells. Insets in each histogram in (A) show the parameters of division index and the percentages of divided cells, as calculated with FlowJo software. The gray line in (B) shows undivided donor cells from nonirradiated mice. Results shown are one (A) or two (B) from four experiments.

Table 1Comparison of PKC $\theta^{-/-}$, PKC $\eta^{-/-}$, and DKO mice. IS, immunological synapse.

	PKCθ KO	PKCη KO[#]	DKO[#]
Thymocytes			
Positive selection	Mildly impaired [#]	Normal	Strongly impaired
Negative selection	Normal	Normal	ND
Mature T cells			
CD4:CD8 T cell ratio	Lower than WT	Higher than WT	Equal to WT
Proliferation			
to α CD3 in vitro	Severely impaired	Mildly impaired	\approx PKC θ KO
to PMA/iono	Normal	Normal	ND
to antigen in vivo	Normal or Impaired	Impaired	ND
to antigen in vitro	Impaired	Impaired	ND
Homeostatic prolif.			
Non-Tg	CD8 Normal	CD8 impaired	Strongly impaired
OT-I Tg	Normal [#]	Impaired	Strongly impaired
Signaling events			
Ca ²⁺ flux	Impaired	Impaired	ND
NF- κ B translocation	Impaired	Impaired	ND
Recruitment to IS [*]	Recruited, central region	Recruited, diffuse pattern	

* Not based on knockout mice.

[#] Based on data obtained from this study. ND: not determined.